ISSN 0006-2979, Biochemistry (Moscow), 2025, Vol. 90, No. 12, pp. 1970-1984 © The Author(s) 2025. This article is an open access publication.
Russian Text © The Author(s), 2025, published in Biokhimiya, 2025, Vol. 90, No. 12, pp. 2077-2092.

Progeroid Syndrome with Signs of Autophagy Dysfunction in the Naked Mole Rat (*Heterocephalus glaber*)

Vasiliy N. Manskikh[1,a]*, Eugene V. Sheval[1], Maria V. Marey[2], Olga A. Averina[1], and Mikhail Yu. Vyssokikh[1,2]

[1]*A. N. Belozersky Research Institute of Physico-Chemical Biology, Lomonosov Moscow State University, 119992 Moscow, Russia*

[2]*V. I. Kulakov National Medical Research Center for Obstetrics, Gynecology, and Perinatology, Ministry of Health of the Russian Federation, 117997 Moscow, Russia*

[a]*e-mail: manskikh@mail.ru*

Received July 1, 2025
Revised November 27, 2025
Accepted November 27, 2025

Abstract—The naked mole rat is considered a unique non-aging mammalian species and is widely used in laboratories to study the biology of longevity. Previously, our group was the first to describe a new fatal disease in the naked mole rat, termed "idiopathic cachexia." A detailed study of pathological changes in the organs of affected animals, combined with the data on gene expression changes, allows us to interpret this disease as a highly specific variant of accelerated aging (progeroid syndrome or progeria) in these animals. Symptoms of the disease include cachexia, cataracts, lipofuscinosis, and appearance of amyloid bodies (corpora amylacea) in the brain, severe degeneration of cardiomyocytes, fatty degeneration, and generalized lipofuscinosis of the liver and kidneys, with signs of autophagy dysfunction in these organs. Further research is needed to elucidate the mechanism of this disease in animals with negligible aging, such as naked mole rats, which may provide insights into the mechanisms of aging and lifespan extension.

DOI: 10.1134/S0006297925601960

Keywords: naked mole rat, autophagy, progeria, aging, lipofuscin

INTRODUCTION

Since the publication of Buffenstein et al. [1], the naked mole rat has been regarded as a mammalian species with negligible or no aging. Indeed, this animal exhibits numerous unique features, including an unusually long lifespan for a rodent (up to 40 years) [1, 2], no increase in mortality risk with age [1-3], resistance to spontaneous and induced carcinogenesis [4-8], many neotenic traits [3], and other physiological characteristics [9, 10]. Without delving into the debate about how much the focus on studying these features is tied to the fascination with a new research subject, and why similar traits are not studied in other animals (for example, resistance to tumor growth in guinea pigs [11]), it must be acknowledged that the naked mole rat is truly a unique model organism for studying gerontology. While physiology of this animal has been extensively studied, its pathology has received relatively little attention – only a few studies have broadly described the spontaneous pathology of the naked mole rat [6, 10, 12-15]. Although several potentially age-related diseases have been identified (progressive rodent nephropathy [13, 16], malignant tumors [6, 14], skin and organ mineralization [12]), in general, the presence of aging-related pathologies in this animal remains poorly studied and rarely debated.

Previously, our research group described a new disease in the naked mole rats, characterized by a sharp decline in body weight, a distinctive external appearance, ascites, neurological symptoms, and

* To whom correspondence should be addressed.

death of the relatively young individuals (2-6 years old). This disease was termed "idiopathic cachexia" [17]. A detailed pathological examination of the deceased and euthanized animals with signs of this disease revealed a range of morphological and histochemical changes traditionally associated with aging at the cellular and tissue levels. This article describes these changes. Since the preliminary data on the microRNA spectrum in these animals indicated altered regulation of gene expression related to autophagy [17], and based on the available morphological data (lipofuscin accumulation), this study investigated markers of this process.

MATERIALS AND METHODS

Animal care. A colony of naked mole rats at the Belozersky Institute of Physico-Chemical Biology, Lomonosov Moscow State University (comprising 54 individuals), was obtained from a core group imported from the Leibniz Institute for Zoo and Wildlife Research (IZW) in Berlin, Germany. All animals described in this study were from the same colony and were housed together in a system of cylindrical plastic containers connected by plastic tubes, at 27 ± 1°C and 50 ± 10% humidity, with a 12/12-hour light/dark cycle (10:00-22:00 light) and atmospheric ventilation. The diet consisted of apples, sweet potatoes, carrots, and grains, provided daily. To enrich the habitat, a rectangular container with high-density clay, mimicking the natural soil of their habitat, was installed. Six months after the container was introduced, some worker animals began to lose weight rapidly. The container was immediately removed after signs of cachexia were detected in 9 out of 54 animals (3 females and 6 males, aged 2-6 years). The animals were then observed for 3 years. To monitor their condition, the body mass index was measured every 4-5 months in both cachexic and healthy control animals of the same age (n = 9; 4 females and 5 males) from the same colony. Euthanasia was performed by decapitation after anesthesia with isoflurane inhalation (5% at 0.4 L/min flow; Laboratorios Karizoo S.A., Spain) using an R500 system (RWD, China).

Necropsy and histopathological examination. Spontaneously deceased (n = 2) and euthanized (n = 7) animals with signs of cachexia underwent pathological examination. The criteria for euthanasia were as follows: 15% reduction in body weight and visual signs of cachexia, ascites, and neurological symptoms (stupor and ataxia). Additionally, 7 healthy control animals without signs of cachexia, kept under the same conditions, were euthanized and examined. All animals underwent thorough macroscopic examination. Samples were taken from the heart, lungs, liver, kidneys, pancreas, mesenteric lymph nodes, spleen, brain, adrenal glands, stomach, large and small intestines, skin, skeletal muscles, thyroid gland, salivary glands, eyes, and reproductive organs.

Organ samples were fixed in a 10% formalin (and in some cases, zinc formalin, Champy's, Carnoy's, and Bouin's mixtures), dehydrated in a 99.7% isopropanol (Biovitrum, Russia), and embedded in a paraffin (Biovitrum), followed by staining with hematoxylin and eosin using a routine protocol [18]. Microscopic examination was performed using an AxioScope A1 microscope (Carl Zeiss, Germany), and microphotographs were taken with an MRc.5 camera (Carl Zeiss).

Identified changes were classified according to the criteria accepted in the pathology of laboratory animals [19-22].

Histochemical examination. Paraffin sections (3 μm) were examined unstained using a fluorescence microscope with a FITC filter (excitation at 493 nm), stained with Sudan IV, Schmorl's method (for lipofuscin), Giemsa, PAS, Warthin–Starry (for bacteria), Van Gieson (for collagen), Altman (for mitochondria), Lepehne–Pickworth (for hemoglobin), Landrum (for intracellular protein granules), Stein, Fouchet (for bilirubin), and Perl's method (for hemosiderin) using routine protocols [18]. Additionally, immunohistochemical examination of the brain was performed using rabbit monoclonal antibodies against beta-amyloid (ab201060; Abcam, USA; dilution 1 : 1000), using standard immunoperoxidase techniques on paraffin sections after heat-induced epitope retrieval in a citrate buffer (pH 6.0), with a detection system (Cell Margue, USA) and appropriate positive and negative controls.

For score assessment of changes, the following criteria were used: hepatic lipofuscinosis (0 – none, 1 – pigment visible in individual hepatocytes, 2 – pigment present in most hepatocytes in the perinuclear zone, 3 – pigment present in all hepatocytes); fatty degeneration (0 – none, 1 – fatty degeneration in individual cells, 2 – involvement of up to 50% of hepatocytes, 3 – involvement of more than 50% of hepatocytes); myocardial degeneration (0 – none, 1 – single foci, 2 – multiple foci, 3 – total involvement); cataract (0 – none, 1 – single subcapsular foci, 2 – involvement of less than 50% of the lens, 3 – involvement of more than 50% of the lens); amyloid deposits in the thalamus (0 – none, 1 – single deposits per section, 2 – single deposits in each 1000× microscope field, 3 – multiple deposits in each field); renal lipofuscinosis (0 – none, 1 – present in individual tubules, 2 – involvement of up to 50% of tubules, 3 – involvement of more than 50% of tubules).

Electron microscopy. Samples of liver and kidney tissues were taken for electron microscopy. Tissue samples (0.5×0.5×1 mm) were fixed in a

Table 1. Gene-specific primers for autophagy marker genes and the reference gene

Gene	Forward primer; Tm (°C)	Reverse primer; Tm (°C)
p62	GCTGTCTGCCCTGTTTTCAT; 58.75	GGCCCAAGTGCTATTCACAG; 58.90
LC3b	AAGAGTGGAAGACGTTCGGC; 60.32	GGTTTTATCCAGGACGGGCA; 60.03
ATG14	AAGCAGAGAGGCAAACTCCC; 59.96	TGTGATCAGCTCTTGGGAACT; 59.02
ATG9a	TGCATGCTCTACGAATCCCC; 59.89	GAAACAGAGAGCCAGGTCCC; 60.04
GAPDH	TGGCAAGGTGGATATCGTGG; 59.82	CTTCTCGTGGTTCACACCCA; 59.89

Note. Tm, melting temperature.

2.5% glutaraldehyde (Sigma, USA) in a cacodylate buffer, post-fixed in 1% OsO_4 (EMS, USA), dehydrated in ethanol and acetone, and embedded in SPI-Pon 812 (Structure Probe, Inc., USA). Ultrathin sections were made using a diamond knife (DiATOME, USA) and mounted on copper slot grids (Ted Pella, USA). Sections were stained with uranyl acetate and lead nitrate and examined using a JEM 1400 electron microscope (JEOL, Japan) at accelerating voltage of 80 kV.

Gene expression analysis of autophagy markers. Liver tissue samples obtained at necropsy (n = 6 for both cachexic and control animals) were mechanically homogenized in liquid nitrogen and lysed in an ExtractRNA reagent (Evrogen, Russia). Total RNA was isolated using a standard method with a guanidine thiocyanate/phenol/chloroform mixture. RNA concentration was determined using a NanoPhotometer (Implen, Munich, Germany) at 260/240 nm. Reverse transcription was performed using a RevertAid First Strand cDNA Synthesis Kit (Thermo Scientific, USA). Quantitative reverse transcription PCR (RT-qPCR) was performed in real-time using a qPCRmix-HS SYBR+LowROX (5X) kit (Evrogen) with gene-specific primers (Evrogen) (Table 1). Primers were selected using the Primer Blast service (https://www.ncbi.nlm.nih.gov/tools/primer-blast/). Primer validation was performed by matching melting temperature (Tm) with the calculated value (provided in Table 1). For negative control, RNA isolated from *Escherichia coli* after reverse transcription was used as a template, as described above. Amplification and detection were performed using a DT Prime 4 amplifier (DNA-Technology, Russia). For all primers, absence of DNA contamination in the isolated RNA samples was confirmed by performing amplification without reverse transcription under the described conditions and parameters. No DNA contamination was detected in the samples. Gene expression analysis was performed using the $2^{-\Delta\Delta Ct}$ method, with *GAPDH* as the reference gene. Results were normalized to the average expression level of *GAPDH*.

Electrophoresis and Western blot analysis. Electrophoresis in 12% polyacrylamide gel was performed using a routine method with minor modifications described previously [23]. Liver tissue fragments obtained at necropsy (n = 3 for both cachexic and control animals) were lysed in a buffer containing: 150 mM NaCl, 50 mM Tris-HCl (pH 8.0), 0.5% Nonidet P-40, 1% sodium deoxycholate, 0.5% sodium dodecyl sulfate, and protease inhibitors (Thermo Fisher Scientific, USA). After separation (30 μg of protein per lane), proteins were electrophoretically transferred to a nitrocellulose membrane (Bio-Rad, USA) and incubated with diluted antibodies using a routine method. Primary antibodies included rabbit monoclonal antibodies against mouse proteins ATG14 (ab315009; dilution 1 : 1000), ATG9a (ab108338; dilution 1 : 1000), and rabbit polyclonal antibodies against mouse proteins p62 (ab91526; concentration 1 μg/mL) [24, 25] and housekeeping protein beta-actin (ab8227; dilution 1 : 2000) [26], obtained from Abcam; and antibodies against LC3b (Cell Signaling, USA; #2775; dilution 1 : 1000) [25]. Dilution was performed as recommended by the manufacturers in a buffer containing 150 mM NaCl, 50 mM Tris-HCl (pH 7.5), 0.1% Tween 20, and 1% bovine serum albumin. Secondary antibodies, conjugated with horseradish peroxidase and specific to rabbit antibodies, were diluted in the same buffer at a ratio of 1 : 20,000 according to the manufacturer's recommendations (ab6721; Abcam). Luminescent signal was visualized using a Novex ECL kit (Invitrogen, USA) and a ChemiDoc scanner (Bio-Rad). Due to the lack of commercially available antibodies against *Heterocephalus glaber* proteins, validation of antibodies against ATG14 and ATG9a, used for the first time, was performed by aligning the peptide antigen sequences used by the companies to produce antibodies against the protein sequences of the naked mole rat, obtained using the online services at https://www.uniprot.org/ and the database at http://naked-mole-rat.org/annotations/details/XP_004871135.1/ and http://naked-mole-rat.org/annotations/details/XP_004864595.1/ for ATG14 and ATG9a, respectively.

In all cases, suitability of the antibodies for the naked mole rat was established by the presence of a single specifically stained band corresponding to the molecular weight and mobility of the protein under study.

Protein concentration determination. Protein concentration in the samples for Western blot analysis was determined using bicinchoninic acid and bovine serum albumin as a standard, following the manufacturer's recommendations (Pierce, USA).

Statistical analysis. Data analysis was performed using GraphPad Prism 8. Data were first tested for Gaussian distribution using the D'Agostino & Pearson omnibus normality test, then analyzed using Student's *t*-test, Mann–Whitney test, or one-way ANOVA. Results are presented as a mean ± standard deviation (SD). Differences were considered significant at $p < 0.05$.

RESULTS

Clinical characteristics of the disease. Clinical manifestations of the disease have been described in detail previously [17]. In all cases, the affected animals were worker individuals. Visually, the animals appeared severely emaciated, with sunken flanks and a pointed snout, resembling appearance of the 30-year-old naked mole rats [9]. Objective examination of animals with signs of cachexia revealed a 15% reduction in the body mass index compared to the control animals from the same colony [17]. Despite this, they exhibited the same feeding behavior as other animals. Immediately before death, the animals displayed neurological symptoms, including stupor or ataxia with rolling onto their backs when attempting to move.

All animals exhibited similar changes, although to varying degrees. At necropsy, signs of cachexia and complete absence of visible fat deposits were noted. The liver was typically dark brown, and a light-yellow transparent fluid (ascites) had accumulated in the abdominal cavity. The kidneys were pale yellow. Other organs were proportionally reduced in size but without visible pathological changes.

Histopathological analysis results. Microphotographs showing structure of the organs in the healthy control naked mole rats, for comparison with the pathologically altered organs, are provided in Fig. 1 due to the rarity of this animal.

Liver. The most severe changes in the affected animals were found in the liver and have been partially described previously [17]. Despite the overall preservation of organ architecture (no signs of lobule deformation or fibrosis), significant changes were observed in hepatocytes and stromal cells. The cytoplasm of hepatocytes contained a large number of light-brown pigment granules that, when treated with osmium tetroxide (Champy's fixation), stained intensely black-brown, green with Giemsa, exhibited strong autofluorescence in paraffin sections, stained weakly with Sudan IV and PAS, did not give a positive Perl's reaction for iron or a reaction for bilirubin, but stained blue-green with Schmorl's method (Fig. 2, a-d). These histochemical properties are characteristic of the "aging pigment" (lipofuscin) [27]. Large amounts of this pigment accumulate in the perinuclear region of cells, which become hypertrophied, binucleated, and have markedly enlarged nucleoli. Hypertrophy of the cells is always localized in the periportal zone of the lobules. In the hypertrophied cells, along with lipofuscin, numerous eosinophilic granules are visible, which stain red with Altman's method (after Champy's fixation), characteristic of mitochondria; and both pigment and mitochondria are concentrated in the perinuclear zone (Fig. 2d). When stained with Lepehne–Pickworth and Landrum, the phagocytosed erythrocytes were occasionally visible in the cytoplasm of individual hypertrophied hepatocytes (Fig. 2e). Some liver cells, on the contrary, undergo atrophy and fatty degeneration with accumulation of large lipid droplets (stained black after fixation with Champy's mixture with OsO_4). Among the hypertrophied hepatocytes, foci of extramedullary hematopoiesis, unusual for the liver of the naked mole rat, are sometimes observed. Kupffer cells (liver macrophages) show strong accumulation of hemosiderin (giving a positive reaction for trivalent iron with Perl's method), reaching a degree characteristic of hemochromatosis (Fig. 2f). These changes were not observed in the animals without signs of cachexia; a species-specific feature of hepatocytes in the healthy naked mole rats is optically clear cytoplasm, due to their high glycogen content (Fig. 1a).

Kidneys. In the kidneys, in addition to calcium phosphate deposits characteristic of all naked mole rats (including those without signs of disease), intracellular deposits of lipofuscin, numerous small lipid droplets in the cells of the proximal tubules, and hemosiderin in the individual tubules were found (Fig. 3, a and b). The renal glomeruli were unchanged. These changes were not found in the kidneys of healthy animals (Fig. 1b).

Heart. Changes in the heart included severe vacuolar degeneration and atrophy of cardiomyocytes in the walls of both ventricles (Fig. 3c), as well as accumulation of a small amount of brown pigment in the individual cardiomyocytes, similar to that found in hepatocytes. The myocardium of healthy animals showed no changes (Fig. 1c).

Eyes. The examined animals exhibited previously undescribed eye lesions. These appeared as typical degeneration of peripheral lens fibers with swelling, clearing, and formation of Morgagnian spheres,

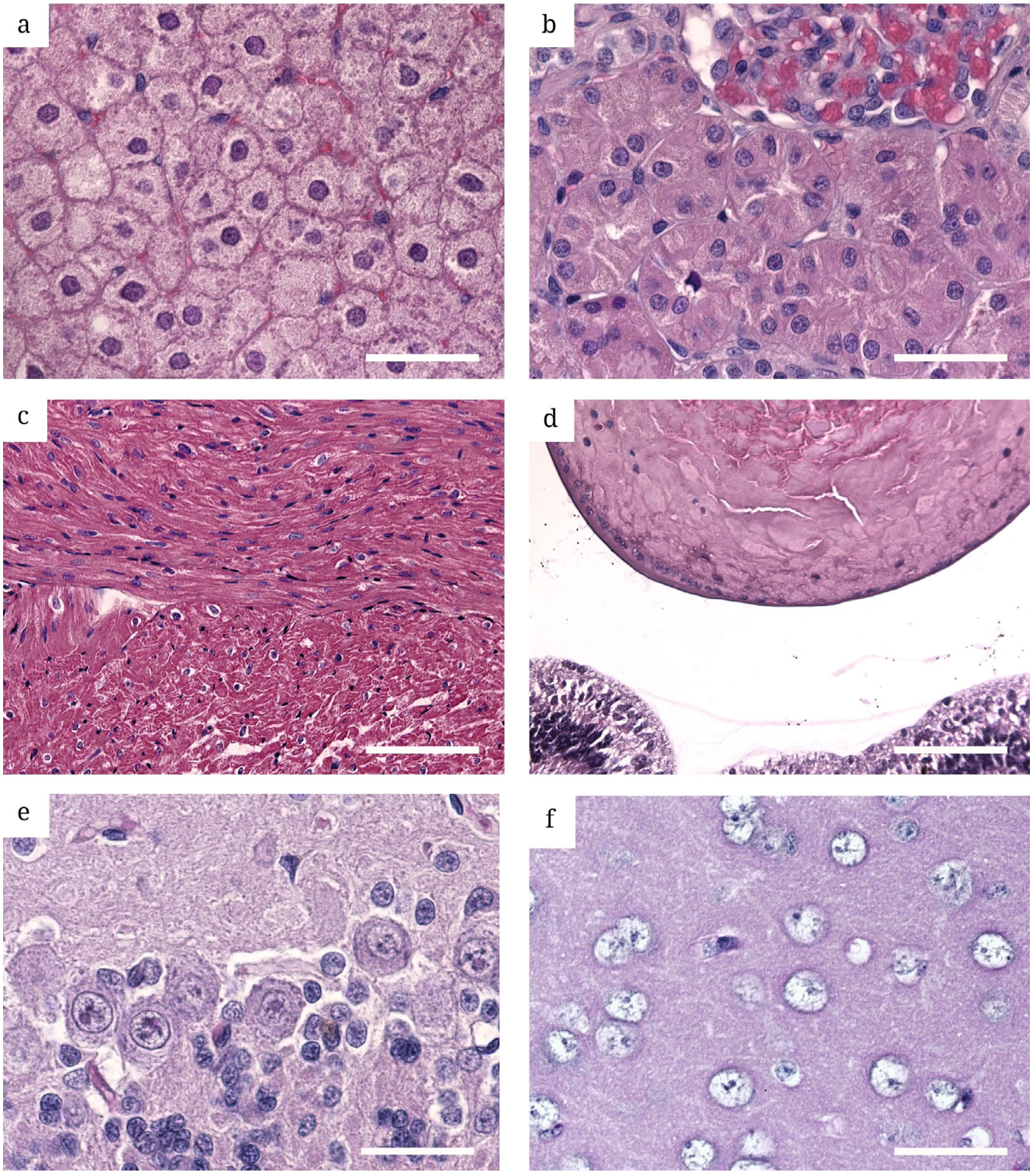

Fig. 1. Histological appearance of internal organs in healthy naked mole rats. a) Liver; b) kidney; c) myocardium; d) eye lens; e) cerebellum; f) thalamus. Staining methods: a-d) hematoxylin and eosin; e) PAS (with hematoxylin counterstain); f) Immunoperoxidase reaction with antibodies against beta-amyloid with PAS and hematoxylin counterstain. Scale bars and magnifications: a, b, e, f) 40 μm, 1000×; c, d) 100 μm, 400×.

characteristic of cataracts (Fig. 3d), but not in the eyes of intact naked mole rats (Fig. 1d). The retina, choroid, cornea, and other eye structures were unchanged.

Brain. Significant changes were found in the brain. The PAS-positive pigment inclusions, similar to those in hepatocytes, were detected in the neurons

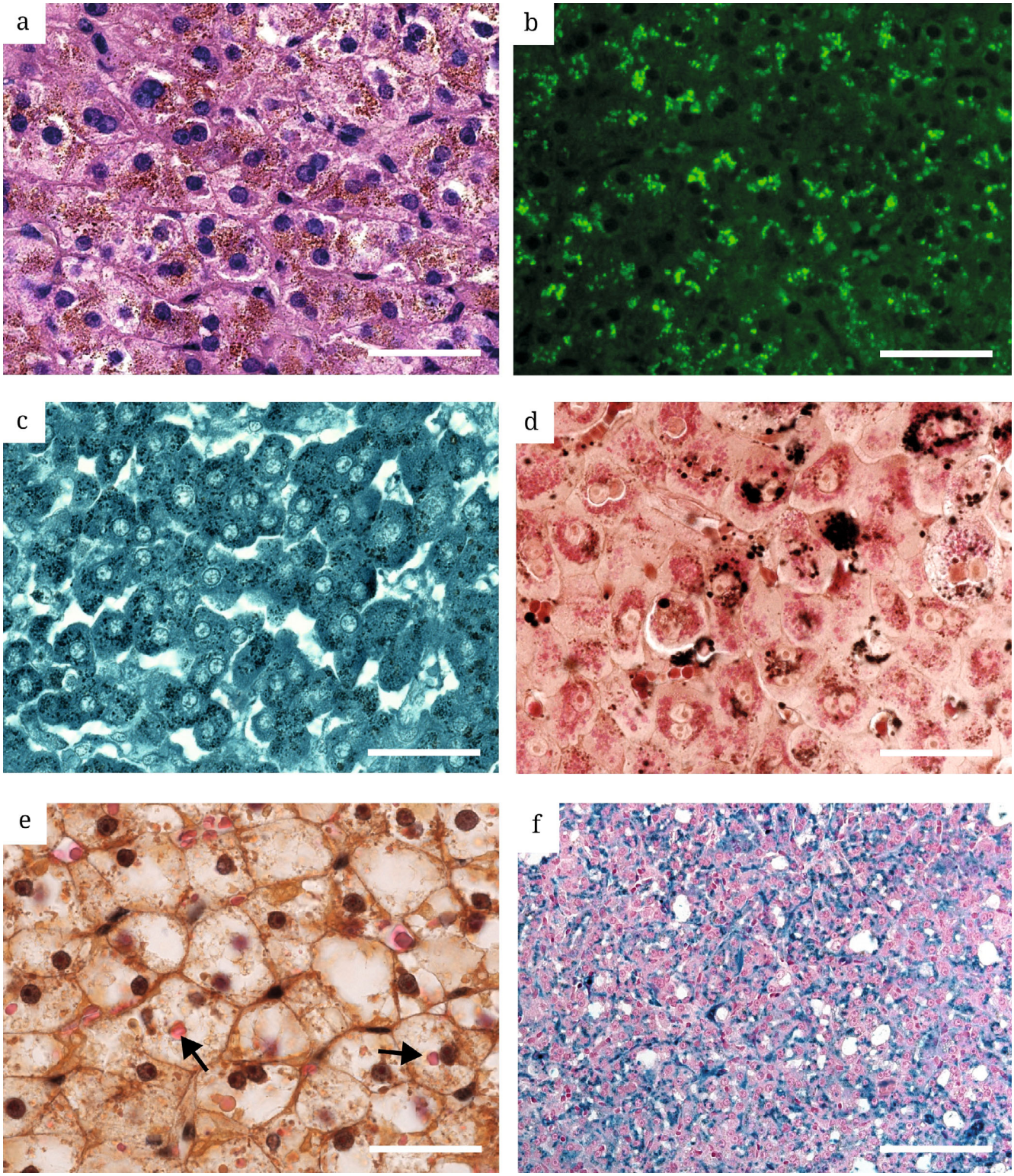

Fig. 2. Changes in the liver of naked mole rats with cachexia. a) A large number of dark brown pigment granules in the cytoplasm of hepatocytes; b) autofluorescence of pigment granules (lipofuscin); c) positive dark blue staining of pigment granules in hepatocytes with Schmorl's method; d) dark brown pigment granules among numerous large mitochondria (pink) concentrated in the perinuclear zone of hepatocytes, black deposits – lipid droplets; e) erythrocytes (pink, arrows) in the cytoplasm of individual hepatocytes; f) intense accumulation of iron-containing pigment (hemosiderin) in Kupffer cells (blue). Scale bars and magnifications: a-e) 40 μm, 1000×; f) 200 μm, 200×. Staining methods: a) Hematoxylin and eosin; b) Unstained paraffin section, FITC filter, excitation at 493 nm; c) Schmorl's reaction; d) Altman's staining after Champy's fixation (with OsO_4); e) Landrum's staining; f) Perl's reaction with nuclear fast red counterstain.

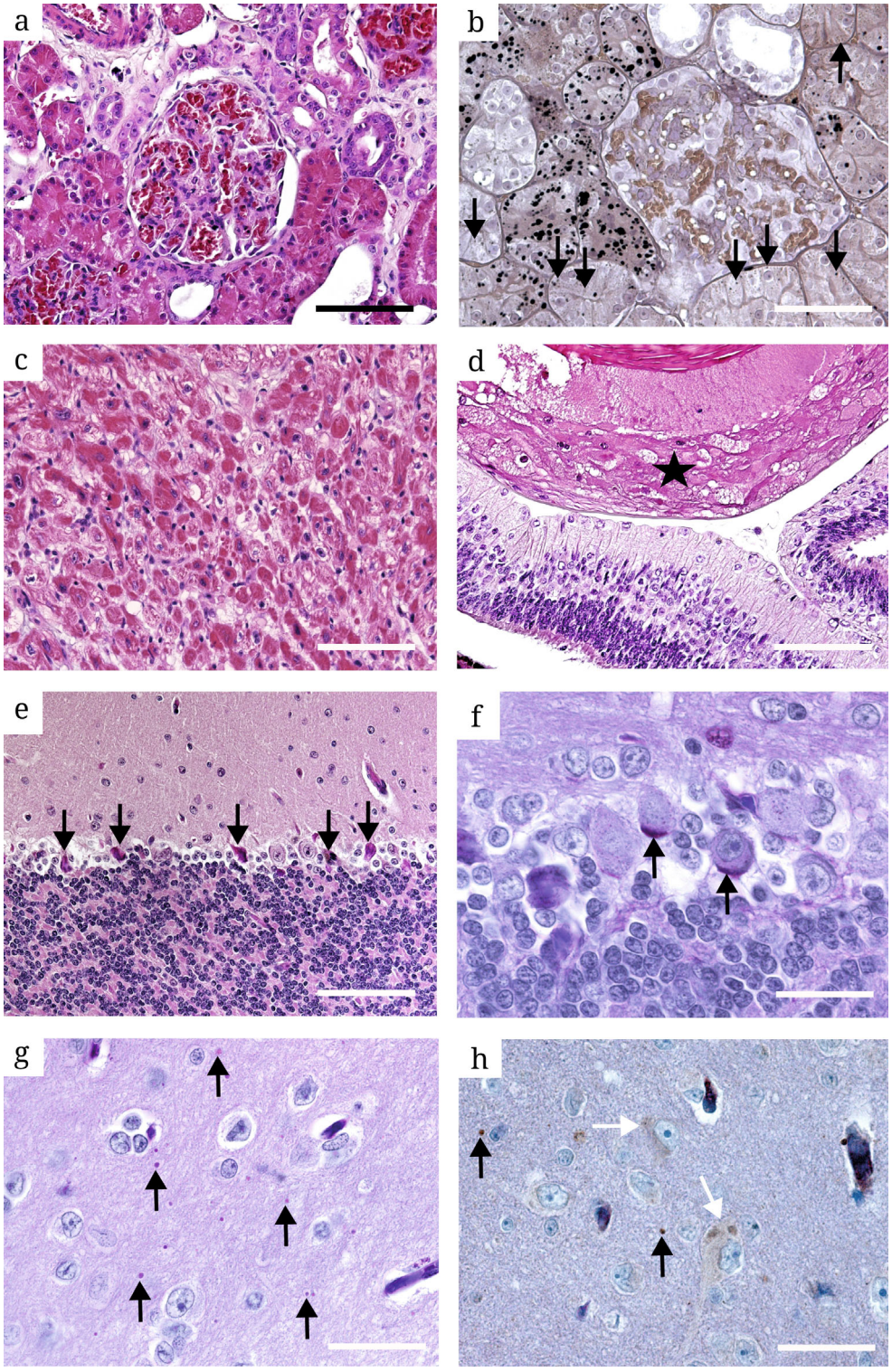

Fig. 3. Changes in various internal organs of naked mole rats with cachexia. a) Unchanged renal glomerulus; b) Numerous granules of lipofuscin (brown) and lipid droplets (black) in the cytoplasm of tubules; c) Severe degenerative changes in the myocardium without inflammatory reaction; d) Cataract, area of lens damage (asterisk) with Morgagnian spheres; e) Degenerative changes in some Purkinje neurons of the cerebellum (arrows); f) PAS-positive deposits of lipofuscin in some Purkinje neurons of the cerebellum (arrows); g) PAS-positive amyloid bodies (corpora amylacea) in the neuropil of the thalamus; h) Positive reaction of intracellular deposits in neurons (white arrows) and amyloid bodies (black arrows) of the thalamus with antibodies against human beta-amyloid. Staining methods: a, c, d, e) Hematoxylin and eosin; b) Hematoxylin after fixation with Champy's mixture (with OsO_4); f, g) PAS reaction with hematoxylin counterstain; h) Immunoperoxidase reaction with antibodies against beta-amyloid with PAS and hematoxylin counterstain. Scale bars and magnifications: a-d) 100 μm, 400×; e-h) 40 μm, 1000×.

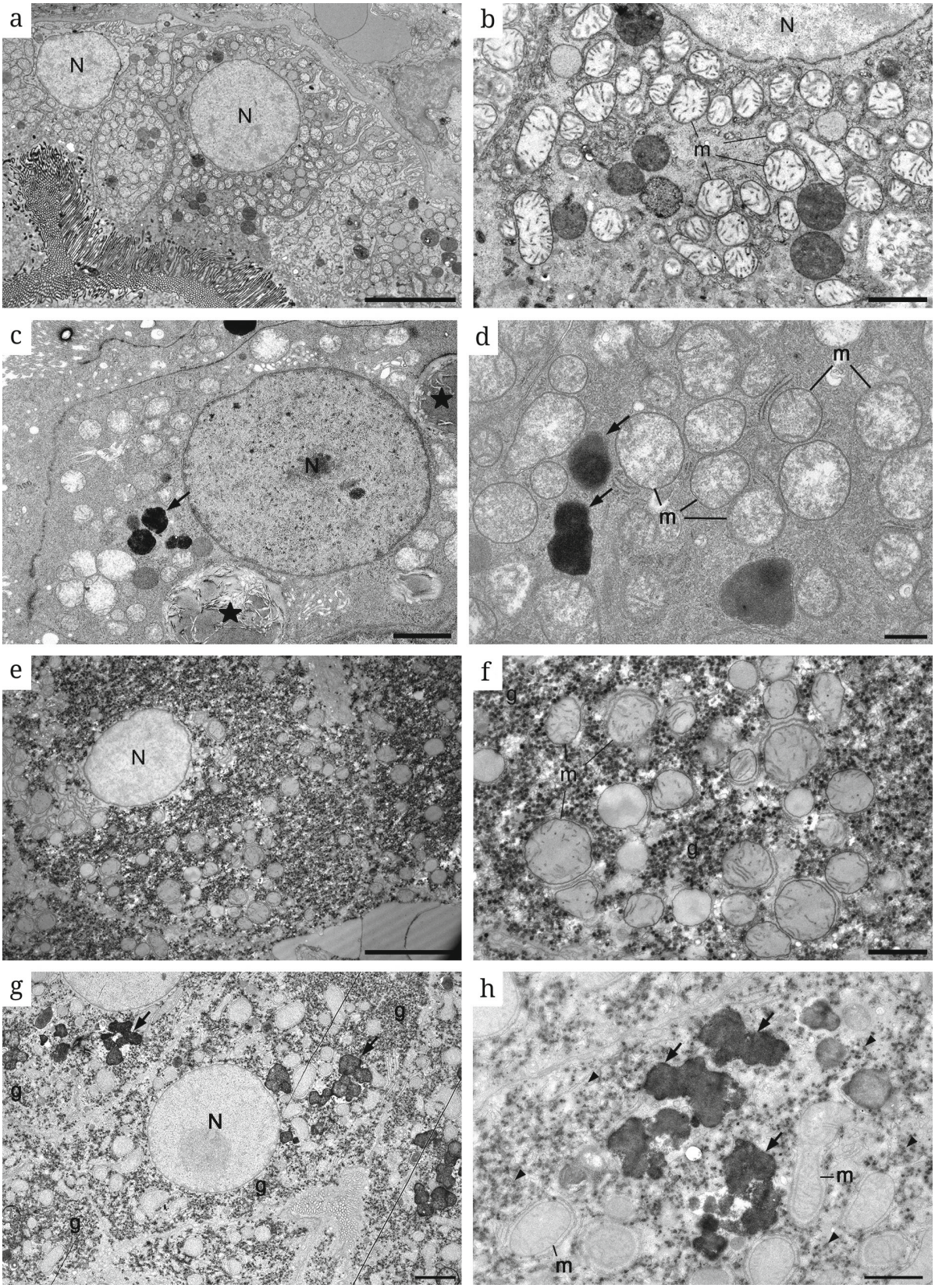

Fig. 4. Ultrastructural changes in the kidney tubule cells and hepatocytes in the animals with cachexia. a, b) Kidney tubule cells of a healthy naked mole rat; c, d) kidney tubule cells of a cachexic naked mole rat; e, f) liver cells of a healthy naked mole rat; g, h) liver cells of a cachexic naked mole rat. N, nuclei; g, glycogen granules; m, mitochondria. Asterisks indicate structures morphologically similar to autophagosomes; arrows indicate lipofuscin granules or their accumulations. Scale bars: a, c, e, g) 2 μm; b, d, f, h) 1 μm.

Table 2. Results of the score assessment of the severity of the most important pathological changes in organs

Group	Hepatic lipofuscinosis	Hepatic fatty degeneration	Myocardial degeneration	Cataract	Amyloid deposits in the thalamus	Renal lipofuscinosis
Control (M ± SD, n = 7)	0	0	0	0 (n = 5)	0	0
Cachexia (M ± SD, n = 9)	2.3 ± 0.7	1.3 ± 0.5	1.6 ± 0.7	1.6 ± 0.8 (n = 5)	2.0 ± 0.9	1.3 ± 0.5

Note. In all cases, $p < 0.01$.

from various regions. Particularly numerous were these inclusions in the Purkinje neurons in the cerebellar cortex, which also showed signs of degeneration, such as eosinophilic shrunken neurons (Fig. 3, e-f). Additionally, vacuolar changes were observed in the neuropil around the third ventricle, and amyloid-like PAS-positive inclusions in the neuropil (corpora amylacea) and PAS-positive granules in the cytoplasm of neurons in various brain regions (Fig. 3g). A particularly large number of amyloid bodies were found in the thalamus and hypothalamus. Staining with antibodies against beta-amyloid did not reveal plaques typical of Alzheimer's disease, but most PAS-positive granules in the cytoplasm of neurons and in the neuropil gave a positive reaction (Fig. 3h). None of these changes were observed in the brains of healthy naked mole rats of the same age (Fig. 1, e-f).

Other organs. It is important to note that histopathological changes in other organs (including skeletal muscles) were not constant and included minimal deposits of brown pigments (lipofuscin, hemosiderin). Bacteria and virus-like inclusions were not found in any organ in any case.

The results of the score assessment of the severity of the most important pathological changes in the organs and tissues are summarized in Table 2.

Electron microscopy examination. *Liver*. Ultrathin sections of the liver of a healthy naked mole rat showed hepatocytes with one or two nuclei (Fig. 4a). Cytoplasm of the cells contained numerous mitochondria and surrounding endoplasmic reticulum components (Fig. 4b). No pathological changes were observed in these organelles. The cytosol was filled with numerous glycogen accumulations, visible only in hepatocytes and absent, for example, in the nearby endothelial cells. Due to the large amount of glycogen, the cytoplasm of hepatocytes appeared dark, and membrane organelles and nuclei appeared lightly stained against this background. In the hepatocytes of cachexic naked mole rats, the same organelles were observed, although the amount of glycogen was visually lower (Fig. 4, c and d). The cells contained single, sometimes quite large (up to 5 μm) lipid droplets. Notably, hepatocytes contained large accumulations of lipofuscin granules (Fig. 4, e and f). These granules always occupied a localized area of the cytoplasm, usually closer to the nucleus. Viral particles and areas of their assembly (viral inclusions) were not detected.

Kidney. For analysis, transverse sections of proximal and distal tubules were selected; for illustration, only photographs of proximal tubules are provided. Epithelial cells forming the walls of the tubules in the kidney of a healthy naked mole rat contained a large number of mitochondria, and no lipofuscin granules were detected (Fig. 4, e and f). In the tubule cells of the cachexic naked mole rats, severely damaged swollen mitochondria were observed, in which cristae were difficult to detect (Fig. 4, g and h). It is important to note that mitochondrial damage in the cells of different tubules varied from minimal to very severe (Fig. 4h). However, in all cases within a single tubule, mitochondria in different cells had approximately the same morphology, i.e., the same level of damage. Large inclusions, possibly autophagosomes, were found in the cells of the proximal tubules. Viral particles and areas of their assembly (viral inclusions) were not detected in either the nuclei or the cytoplasm of the cells.

Expression of autophagy marker genes and proteins. To study autophagy in the liver of the naked mole rat, four marker proteins were selected: ATG9a, ATG14, p62, and the LC3II/LC3I ratio. Classical markers for assessing autophagic flux activity are decrease in p62 (degraded in autophagosomes) and increase in the relative content of the lipidated form of LC3 (LC3II), whose accumulation depends on formation of autophagosomes. ATG14 and ATG9a are additional marker proteins known to be involved in the processes of initiation and elongation of phagophore membranes, closure of autophagosome, and delivery of endosomal material to lysosomes.

Analysis of the content of autophagy marker proteins in the liver tissues by immunoblotting showed a significant increase in the content of p62, ATG14, and ATG9a proteins (Fig. 5) and decrease in the LC3II/LC3I ratio.

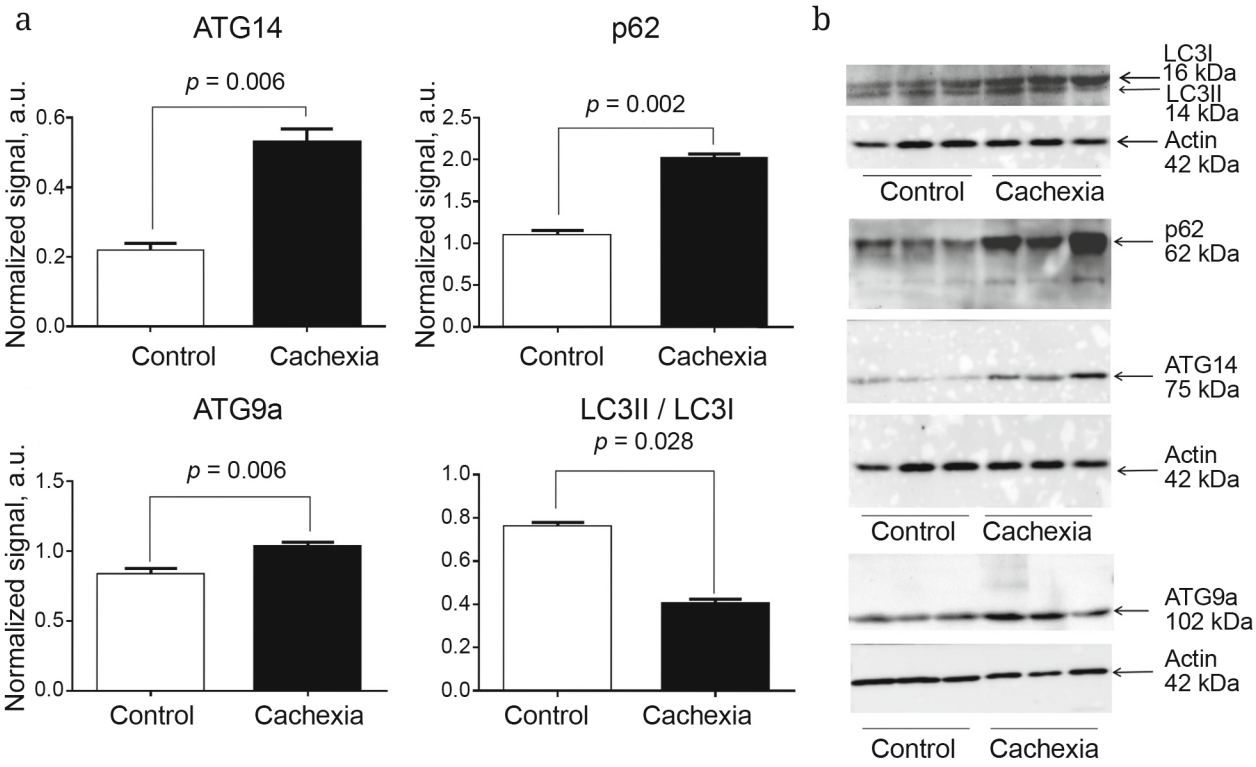

Fig. 5. Changes in the relative content of autophagy marker proteins ATG14, ATG9a, p62, and the LC3II/LC3I ratio in the liver tissue of cachexic animals compared to the normal naked mole rats. a) Diagrams showing a significant (in all cases, $p < 0.05$) increase in the content of proteins (in arbitrary units, normalized to beta-actin) ATG14, ATG9a, p62, and a decrease in the LC3II/LC3I ratio. b) Photographs of individual electropherograms of autophagy marker proteins ATG14, ATG9a, p62, LC3II, LC3I, and housekeeping protein beta-actin from the liver of healthy and cachexic animals.

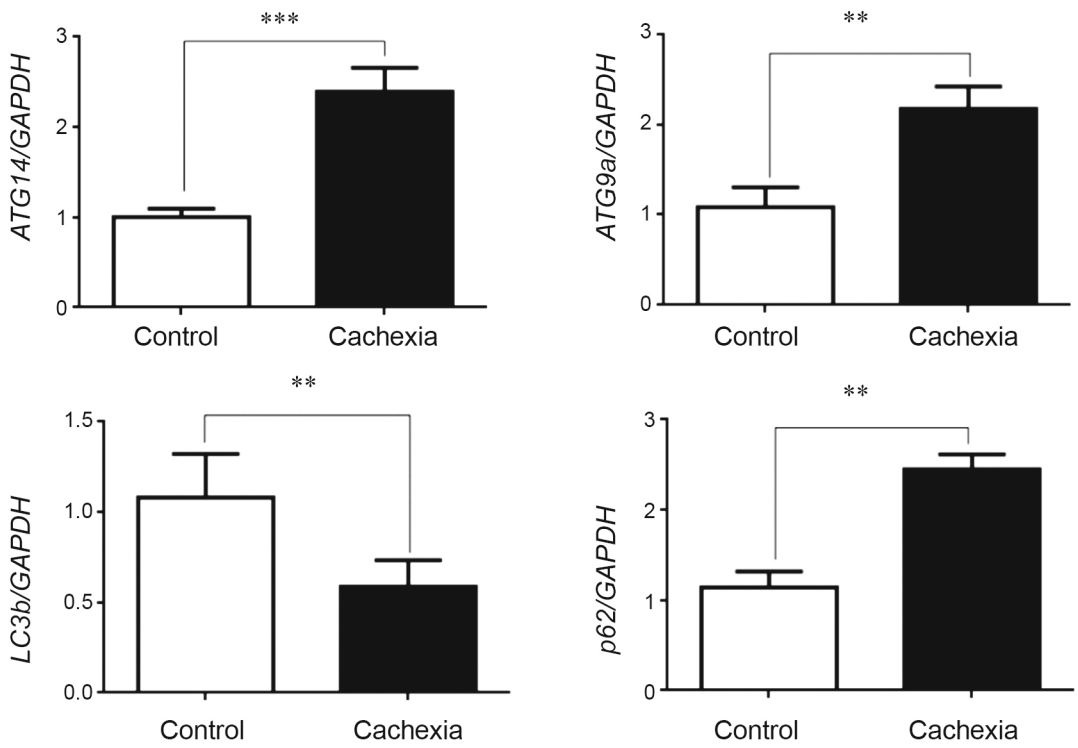

Fig. 6. Relative expression of mRNA of the *ATG14*, *ATG9a*, *LC3b*, and *p62* genes in the liver tissue for cachexic and normal animals. Data represent the mean value of $2^{-\Delta\Delta Ct}$ in the group ± SD; ** $p < 0.01$; *** $p < 0.001$.

Using quantitative PCR, a significant increase in the expression levels of the *p62*, *ATG14*, and *ATG9a* genes and a significant decrease in the mRNA level for *LC3b* in the liver tissue of cachexic animals compared to the normal animals were revealed (Fig. 6).

DISCUSSION

From the detailed description of the pathological changes found in the organs of naked mole rats with signs of the disease, it is clear that this disease, previously designated by us as "idiopathic cachexia," does not resemble any known disease of laboratory rodents [19-22], including pathological conditions known in the naked mole rat [12-15]. Recently, in the study of brain samples from the naked mole rats aged 5-27 years, changes similar to those observed in our animals were described [28], but the authors did not mention the results of examining other organs in these animals or the symptoms observed during life. The pathological changes we found explain clinical picture of the disease well. Massive damage to the kidneys, myocardium, and especially liver could explain the weight loss (cachexia) and ascites found during macroscopic examination. Damage to the cerebellar neurons explains ataxia (inability to maintain posture) observed during the animals' lifetime. Damage to the myocardium and brain was severe enough to lead to the animals' death. No signs indicating an infectious nature of the disease were found during careful examination.

The study of molecular markers provided some information about the processes that may be associated with the morphological changes described in this article. Previously, we showed that in the liver of cachexic animals, the expression level of microRNA nmr-miR-15b-5p, whose targets include mRNAs of proteins such as ATG14 and ATG9a [17], significantly decreases. These proteins are important components of the autophagy cascade [29]. It has been established that regulation of the expression of the *ATG14* and *ATG9a* genes by small non-coding RNA of the miR-15-5p family is significant, particularly for the age-related pathology such as non-alcoholic fatty liver disease, in which a decrease in the level of this microRNA is observed [30]. In this study, we analyzed the content of protein products of the genes responsible for autophagy and their mRNA in the liver of sick naked mole rats. These data show that the expression levels of several genes increased, while the expression level of the *LC3b* gene decreased sharply. The product of this gene plays a key role in the normal autophagic flux, ensuring both capture of material for degradation by the phagophore and closure of the phagophore membranes and formation of the autophagosome [31, 32]. Consequently, deficiency of this protein should lead to autophagy dysfunction already at the stage of phagophore formation and expansion. Although we detected structures resembling autophagosomes, a significant decrease in the LC3II/LC3I ratio serves as a clear indication of the defect in their formation and decrease in autophagic flux. In this regard, increase in the content of the p62 protein in the cells, which is usually degraded in autophagosomes along with its marked targets [31-33], could be associated not so much with its hyperexpression as with the reduced degradation. It is important to note that the increase in the p62 protein has already been described as a marker of autophagy disorders during aging [34]. The increase in expression and content of other proteins responsible for initiation and elongation of phagophore membranes (ATG9a, ATG14) [31] could be a cellular compensatory reaction to ineffective autophagy. Another evidence of defective autophagy is accumulation of lipofuscin in cells, which indicates inefficiency of another stage of this process – lysosomal degradation. Thus, along with the increase in factors responsible for the initiation of autophagy, there are signs of its clear dysfunction and inefficiency at the subsequent stages. Elucidating the causes of such complex dysfunction requires additional research. However, it is important to note that autophagy disorders (blockade of ATG9a–Fam134b–LC3β and ATG9a–Sec62–LC3β interactions, as well as impaired reticulophagy – autophagic processing of the endoplasmic reticulum) have already been described as a mechanism leading to the development of a progeroid phenotype in mice [35].

In summary, the following conclusion could be drawn about the nature of the disease we observed in naked mole rats. The dominant changes in the histopathological picture of the disease are generalized lipofuscinosis in the liver, kidneys, brain, and, to a lesser extent, the myocardium, which is accompanied by severe emaciation (making sick animals resemble 30-year-old naked mole rats), the appearance of amyloid bodies (corpora amylacea) in the brain, and the development of cataracts in the lens. All such changes are classified as characteristic of aging, and therefore, the disease we previously described as "idiopathic cachexia" (the term "idiopathic" refers to diseases of unclear etiology) could be classified as a type of progeria or progeroid syndrome. The results of studying marker genes and proteins LC3b, p62, ATG9a, ATG14, together with morphological signs (detection of numerous lipofuscin granules and lipid droplets by light microscopy and autophagosomes by electron microscopy), suggest that in this case, there is a dysfunction of autophagy [36, 37] accompanied by the hyper-expression and hyper-activation of some of its factors and pathways

and deficiency of the others. Therefore, the discovered disease could be called “progeroid syndrome with signs of autophagy dysfunction.” In this case, it should be noted that the disruption of autophagy processes may be either the cause of fatal changes in the organs and tissues of animals or only one of the pathogenetic components, which, nevertheless, is a significant feature of this disease. The cause of the development of this progeroid state, as we previously suggested [17], may be an inadequate activation of metabolism (with a sharp excess of catabolism over anabolism) when animals are under normoxic conditions (21% oxygen, while the usual content for natural colonies is 8-16%). Possibly, this is associated with the long-term effects of oxidative stress developed under normoxia against the background of constant heavy physical exertion (all cachexic animals belong to the group of workers engaged in digging tunnels in dense clay to obtain food delivered to other members of the colony).

It is important to compare this disease with other conditions in humans and animals that are considered progerias. Unfortunately, despite the availability of a significant amount of information on the molecular mechanisms of progeria in humans, morphological changes in the organs of such patients have been poorly studied – there are only few reports of such studies [38, 39]. There is also little data on progeria in the laboratory animals [40]. Analysis of information on the changes in the Werner’s disease and especially Hutchinson–Gilford syndrome shows that these genetic diseases have symptoms both coinciding with the course of natural aging and sharply differing from it. For example, the characteristic deformation of the skull, agenesis of the clavicle, scleroderma-like skin changes, and hypognathia in the Hutchinson–Gilford progeria are not typical of normal aging, and the spectrum of tumors in the Werner’s syndrome is not similar to that known for the elderly [39]. Pathology of natural aging in the laboratory rodents, and, in particular, in mice, differs radically from the human aging. Mice do not develop type 2 diabetes, atherosclerosis (and associated ischemic brain and heart damage), or Alzheimer’s disease, but they do exhibit emaciation, lipofuscinosis, hair loss, atrophy of lymph nodes and spleen, cataracts, and cardiomyopathy [22]. Mouse lines with mutations considered as genetic models of progeria have extremely diverse and dissimilar phenotypes, often affecting some tissues and not others [40]. For obvious reasons, we cannot say to what extent the changes we observe correspond to the pathology of “normal aging” in an animal such as the naked mole rat, but they are quite consistent with those by which mutant mice are classified as models of progeria [40]. At the same time, the age-related signs such as hair loss, atrophic changes in the gonads, or atrophy of lymph nodes and spleen cannot be registered in the naked mole rat due to its anatomical features (lack of hair and atrophic changes in the gonads and lymphoid tissue in the normal young worker animals) [10]. The difference between the disease we described and classical progerias in humans is that their manifestation depends only on the genotype, without provoking factors, or rather, such factors are unknown. However, in the case of autophagic progeroid syndrome, the genetic factor is obviously significant, since it was noted only in a small part of the animals. It is possible that we are dealing with, conditionally speaking, a “reverse mutation,” restoring the type and rate of aging characteristic of all other rodents in the naked mole rat.

CONCLUSION

Thus, in an animal with negligible aging – the naked mole rat – a condition was discovered that, based on a number of signs, could be attributed to the phenomena of accelerated aging (progeroid syndromes or progeria). The exact mechanism of this process requires further study, but our data indicate autophagy dysfunction as a possible pathogenetic mechanism of this syndrome.

STUDY LIMITATIONS

The limitations of this study include the following circumstances mainly associated with working with such a unique animal as the naked mole rat: relatively small size of the studied sample, inability to definitively prove a causal relationship between the identified autophagy disorders and all the described morphological manifestations of the progeroid phenotype, and retrospective nature of the studies.

Contributions

V. N. Manskikh and M. Yu. Vyssokikh – concept and supervision of the work; V. N. Manskikh, E. V. Sheval, M. V. Marey, and O. A. Averina – conducting the study (O. A. Averina – animal observation, V. N. Manskikh – histopathological analysis, E. V. Sheval – electron microscopy, M. V. Marey – analysis of gene and protein marker expression of autophagy); V. N. Manskikh – writing the text; E. V. Sheval and M. Yu. Vyssokikh – editing the text of the article.

Funding

This work was financially supported by the Ministry of Science and Higher Education of the Russian Federation (Agreement no. 075-15-2025-489).

Ethics approval and consent to participate
All applicable international, national, and/or institutional guidelines for the care and use of animals were followed. The study protocol was approved by the Ethics Committee of the Belozersky Institute of Physico-Chemical Biology, Lomonosov Moscow State University (Protocol 2/20 dated 16.11.2022).

Conflict of interest
The authors of this work declare that they have no conflicts of interest.

REFERENCES

1. Buffenstein, R. (2005) The naked mole-rat: a new long-living model for human aging research, *J. Gerontol. A Biol. Sci. Med. Sci.*, **60**, 1369-1377, https://doi.org/10.1093/gerona/60.11.1369.
2. Buffenstein, R. (2008) Negligible senescence in the longest living rodent. the naked mole rat: insights from a successfully aging species, *J. Comp. Physiol.*, **178**, 439-445, https://doi.org/10.1007/s00360-007-0237-5.
3. Skulachev, V. P., Holtze, S., Vyssokikh, M. Y., Bakeeva, L. E., Skulachev, M. V., Markov, A. V., Hildebrandt, T. B., and Sadovnichii, V. A. (2017) Neoteny, prolongation of youth: from naked mole rats to "naked apes" (humans), *Physiol. Rev.*, **97**, 699-720, https://doi.org/10.1152/physrev.00040.2015.
4. Liang, S., Mele, J., Wu, Y., Buffenstein, R., and Hornsby, P. J. (2010) Resistance to experimental tumorigenesis in cells of a long-lived mammal, the naked mole-rat (*Heterocephalus glaber*), *Aging Cell*, **9**, 626-635, https://doi.org/10.1111/j.1474-9726.2010.00588.x.
5. Miyawaki, S., Kawamura, Y., Oiwa, Y., Shimizu, A., Hachiya, T., Bono, H., Koya, I., Okada, Y., Kimura, T., Tsuchiya, Y., Suzuki, S., Onishi, N., Kuzumaki, N., Matsuzaki, Y., Narita, M., Ikeda, E., Okanoya, K., Seino, K., Saya, H., Okano, H., and Miura, K. (2016) Tumour resistance in induced pluripotent stem cells derived from naked mole-rats, *Nat. Commun.*, **7**, 11471, https://doi.org/10.1038/ncomms11471.
6. Delaney, M. A., Ward, J. M., Walsh, T. F., Chinnadurai, S. K., Kerns, K., Kinsel, M. J., and Treuting, P. M. (2016) Initial case reports of cancer in naked mole-rats (*Heterocephalus glaber*), *Vet. Pathol.*, **53**, 691-696, https://doi.org/10.1177/0300985816630796.
7. Gorbunova, V., Seluanov, A., Zhang, Z., Gladyshev, V. N., and Vijg, J. (2014) Comparative genetics of longevity and cancer: insights from long-lived rodents, *Nat. Rev. Genet.*, **15**, 531-540, https://doi.org/10.1038/nrg3728.
8. Oka, K., Fujioka, S., Kawamura, Y., Komohara, Y., Chujo, T., Sekiguchi, K., Yamamura, Y., Oiwa, Y., Omamiuda-Ishikawa, N., Komaki, S., Sutoh, Y., Sakurai, S., Tomizawa, K., Bono, H., Shimizu, A., Araki, K., Yamamoto, T., Yamada, Y., Oshiumi, H., and Miura, K. (2022) Resistance to chemical carcinogenesis induction via a dampened inflammatory response in naked mole-rats, *Commun. Biol.*, **5**, 287, https://doi.org/10.1038/s42003-022-03241-y.
9. Edrey, Y. H., Hanes, M., Pinto, M., Mele, J., and Buffenstein, R. (2011) Successful aging and sustained good health in the naked mole rat: a long-lived mammalian model for biogerontology and biomedical research, *ILAR J.*, **52**, 41-53, https://doi.org/10.1093/ilar.52.1.41.
10. Buffenstein, R., Park, T., Hanes, M., and Artwohl, J. E. (2012) Naked mole rat, In *The Laboratory Rabbit Guinea Pig, Hamster, Other Rodents*, Elsevier, Amsterdam, pp. 1055-1074, https://doi.org/10.1016/B978-0-12-380920-9.00045-6.
11. Manskikh, V. N. (2010) Resistance of guinea pigs to tumor growth: the reality of the phenomenon and its possible causes [in Russian], *Vopr. Oncol.*, **56**, 514-520.
12. Delaney, M. A., Nagy, L., Kinsel, M. J., and Treuting, P. M. (2013) Spontaneous histologic lesions of the adult naked mole rat (*Heterocephalus glaber*): a retrospective survey of lesions in a zoo population, *Vet. Pathol.*, **50**, 607-621, https://doi.org/10.1177/0300985812471543.
13. Delaney, M. A., Kinsel, M. J., and Treuting, P. M. (2016) Renal pathology in a nontraditional aging model: the naked mole-rat (*Heterocephalus glaber*), *Vet. Pathol.*, **53**, 493-503, https://doi.org/10.1177/0300985815612557.
14. Manskikh, V. N., Averina, O. A., and Nikiforova, A. I. (2017) Spontaneous and experimentally induced pathologies in the naked mole rat (*Heterocephalus glaber*), *Biochemistry (Moscow)*, **82**, 1504-1512, https://doi.org/10.1134/S0006297917120094.

15. Delaney, M. A., Imai, D. M., and Buffenstein, R. (2021) Spontaneous disease and pathology of naked mole-rats, *Adv. Exp. Med. Biol.*, **1319**, 353-380, https://doi.org/10.1007/978-3-030-65943-1_15.
16. Manskikh, V. N. (2015) Chronic progressive nephropathy in rodents as a disease caused by an expanding somatic mutant clone, *Biochemistry (Moscow)*, **80**, 582-585, https://doi.org/10.1134/S0006297915050090.
17. Adrianov, M. A., Bobrov, M., Mamedov, I., Manskikh, V., Sheval, E. V., Rachkova, A. A., Shelechova, A. M., Eldarov, C. M., Averina, O. A., and Vyssokikh, M. Y. (2025) A set of microRNAs are differentially expressed in cachexic naked mole rat colony members after chronic heavy burden under normoxia, *Biochimie*, **232**, 83-90, https://doi.org/10.1016/j.biochi.2025.01.010.
18. Suvarna, K., Layton, C. and Bancroft, J. D. (2019) *Bancrofts Theory and Practice of Histological Techniques*, 9th Edn, Elsevier.
19. Tucker, M. J. (1997) *Diseases of the Wistar Rat*, Taylor and Francis, London, https://doi.org/10.4324/9780203211250.
20. Maronpot, R. R. (1999) *Pathology of the Mouse*, Cache River Press, Vienna, IL.
21. Percy, D. H., Griffey, S. M., and Barthold, S. W. (2016) *Pathology of Laboratory Rodents and Rabbits*, Wiley-Blackwell.
22. Mohr, U. (1996) *Pathobiology of Aging Mouse*, Vols. 1/2, ILSI Press.
23. Vyssokikh, M. Yu., Vigovskiy, M. A., Philippov, V. V., Boroday, Ya. R., Marey, M. V., Grigorieva, O. A., Vepkhvadze, T. F., Kurochkina, N. S., Manukhova, L. A., Efimenko, A. Yu., Popov, D. V., and Skulachev, V. P. (2024) Age-dependent changes in the production of mitochondrial reactive oxygen species in human skeletal muscle, *Biochemistry (Moscow)*, **89**, 299-312, https://doi.org/10.1134/S0006297924020093.
24. Du, J., Liu, W., Li, M., Li, Z., Li, X., Dai, Y., Liu, G., Wang, X., Zhu, P., Gladyshev, V. N., and Zhou, X. (2024) Comparative time-series multi-omics analyses suggest H1.2 involvement in anoxic adaptation and cancer resistance, *PLoS Biol.*, **22**, e3002778, https://doi.org/10.1371/journal.pbio.3002778.
25. Kim, J., Chee, W.-Y., Yabuta, N., Kajiwara, K., Nada, S., and Okada, M. (2020) Atg5-mediated autophagy controls apoptosis/anoikis via p53/Rb pathway in naked mole-rat fibroblasts, *Biochem. Biophys. Res. Commun.*, **528**, 146-153, https://doi.org/10.1016/j.bbrc.2020.05.083.
26. Zhao, S., Li, L., Wang, S., Yu, C., Xiao, B., Lin, L., Cong, W., Cheng, J., Yang, W., Sun, W., and Cui, S. (2016) H_2O_2 treatment or serum deprivation induces autophagy and apoptosis in naked mole-rat skin fibroblasts by inhibiting the PI3K/Akt signaling pathway, *Oncotarget*, **7**, 84839-84850, https://doi.org/10.18632/oncotarget.13321.
27. Maranni, E., Usunoff, K. G., and Feirabend, N. K. P. (2009) Lipofuscin and lipofuscinosis, *Encyclopedia Neurosci.*, **2009**, 481-486, https://doi.org/10.1016/B978-008045046-9.00126-1.
28. Ward, J. M., Cartoceti, A. N., and Delaney, M. A. (2021) Brain lesions in aging zoo-housed naked mole-rats (*Heterocephalus glaber*), *Vet Pathol.*, **58**, 142-146, https://doi.org/10.1177/0300985820969982.
29. Suzuki, K., Kubota, Y., Sekito, T., and Ohsumi, Y. (2007) Hierarchy of Atg proteins in pre-autophagosomal structure organization, *Genes Cells*, **12**, 209-218, https://doi.org/10.1111/j.1365-2443.2007.01050.x.
30. Orsi, A., Razi, M., Dooley, H. C., Robinson, D., Weston, A. E., Collinson, L. M., and Tooze, S. A. (2012) Dynamic and transient interactions of Atg9 with autophagosomes, but not membrane integration, are required for autophagy, *Mol. Biol. Cell.*, **23**, 1860-1873, https://doi.org/10.1091/mbc.E11-09-0746.
31. Klionsky, D. J., Petroni, G., Amaravadi, R. K., Baehrecke, E. H., Ballabio, A., Boya, P., Bravo San Pedro, J. M., Cadwell, K., Cecconi, F., Choi, A. M. K., Choi, M. E., Chu, C. T., Codogno, P., Colombo, M. I., Cuervo, A. M., Deretic, V., Dikic, I., Elazar, Z., Eskelinen, E.-L., Fimia, G. M., Gewirtz, D. A., Green, D. R., Hansen, M., Jäättelä, M., Johansen, T., Juhász, G., Karantza, V., Kraft, C., Kroemer, G., Ktistakis, N. T., Kumar, S., Lopez-Otin, C., Macleod, K. F., Madeo, F., Martinez, J., Meléndez, A., Mizushima, N., Münz, C., Penninger, J. M., Perera, R. M., et al. (2021) Autophagy in major human diseases, *EMBO J.*, **40**, e108863, https://doi.org/10.15252/embj.2021108863.
32. Klionsky, D. J., Abdel-Aziz, A. K., Abdelfatah, S., Abdellatif, M., Abdoli, A., Abel, S., Abeliovich, H., Abildgaard, M. H., et al. (2021) Guidelines for the use and interpretation of assays for monitoring autophagy (4^{th} edition), *Autophagy*, **17**, 1-382, https://doi.org/10.1080/15548627.2020.1797280.
33. Viiri, J., Amadio, M., Marchesi, N., Hyttinen, J. M. T., Kivinen, N., Sironenm, R., Rillam, K., Akhtar, S., Provenzani, A., D'Agostino, A. G., Govoni, S., Pascale, A., Agostini, H., Petrovski, G., Salminen, A., and Kaarniranta, K. (2013) Autophagy activation clears ELAVL1/HuR-mediated accumulation of SQSTM1/p62 during proteasomal inhibition in human retinal pigment epithelial cells, *PLoS One*, **8**, e69563, https://doi.org/10.1371/journal.pone.0069563.
34. Sakuma, K., Kinoshita, M., Ito, Y., Aizawa, M., Aoi, W., and Yamaguchi, A. (2015) 3p62/SQSTM1 but not LC3 is accumulated in sarcopenic muscle of mice, *J. Cachexia Sarcopenia Muscle*, **7**, 204-212, https://doi.org/10.1002/jcsm.12045.
35. Peng, Y., Shapiro, S. L., Banduseela, V. C., Dieterich, I. A., Hewitt, K. J., Bresnick, E. H., Kong, G., Zhang, J., Schueler, K. L., Keller, M. P., Attie, A. D., Hacker, T. A., Sullivan, R., Kielar-Grevstad, E., Arriola Apelo, S. I., Lamming, D. W., Anderson, R. M., and Puglielli, L. (2018)

Increased transport of acetyl-CoA into the endoplasmic reticulum causes a progeria-like phenotype, *Aging Cell*, **17**, e12820, https://doi.org/10.1111/acel.12820.
36. Sulzer, D., Mosharov, E., Talloczy, Z., Zucca, F. A., Simon, J. D., and Zecca, L. (2008) Neuronal pigmented autophagic vacuoles: lipofuscin, neuromelanin, and ceroid as macroautophagic responses during aging and disease, *J. Neurochem.*, **106**, 24-36, https://doi.org/10.1111/j.1471-4159.2008.05385.x.
37. Song, S. B., Shim, W., and Hwang, E. S. (2023) Lipofuscin granule accumulation requires autophagy activation, *Mol. Cells*, **46**, 486-495, https://doi.org/10.14348/molcells.2023.0019.
38. Reichel, W., and Garcia-Bunuel, R. (1970) Pathologic findings in progeria: myocardial fibrosis and lipofuscin pigment, *Am. J. Clin. Pathol.*, **53**, 243-253, https://doi.org/10.1093/ajcp/53.2.243.
39. Burtner, C. R., and Kennedy, B. K. (2010) Progeria syndromes and ageing: what is the connection? *Nat. Rev. Mol. Cell Biol.*, **11**, 567-578, https://doi.org/10.1038/nrm2944.
40. Harkema, L., Youssef, S. A., and de Bruin, A. (2016) Pathology of mouse models of accelerated aging, *Vet. Pathol.*, **53**, 366-389, https://doi.org/10.1177/0300985815625169.